New Journal of Physics
The open-access journal for physics

Low-voltage control of ferromagnetism in a semiconductor p–n junction

M H S Owen[1,2,5], J Wunderlich[2,3], V Novák[3], K Olejník[3], J Zemen[3], K Výborný[3], S Ogawa[2], A C Irvine[1], A J Ferguson[1], H Sirringhaus[1] and T Jungwirth[3,4]

[1] Microelectronics Research Centre, Cavendish Laboratory, University of Cambridge, Cambridge CB3 0HE, UK
[2] Hitachi Cambridge Laboratory, Cambridge CB3 0HE, UK
[3] Institute of Physics, ASCR v.v.i., Cukrovarnická 10, 162 53 Praha 6, Czech Republic
[4] School of Physics and Astronomy, University of Nottingham, Nottingham NG7 2RD, UK
E-mail: mhso2@cam.ac.uk

New Journal of Physics **11** (2009) 023008 (9pp)
Received 27 October 2008
Published 4 February 2009
Online at http://www.njp.org/
doi:10.1088/1367-2630/11/2/023008

Abstract. Controlling the magnetization by low-voltage charge depletion in field-effect transistors has been a formidable challenge due to the typically large carrier concentrations in ferromagnets compared to semiconductors. Here we demonstrate that this concept is viable in an all-semiconductor, p–n junction transistor utilizing a thin-film ferromagnetic (Ga,Mn)As channel. We report gate-dependent Curie temperature and magnetoresistance, and persistent magnetization switchings induced by short electrical pulses of a few volts.

[5] Author to whom any correspondence should be addressed.

Contents

1. Introduction

One of the major driving forces in spintronic research is to allow the field to progress from sensors and memories to logic devices, which requires development of three-terminal spintronic transistors. Ferromagnetic semiconductors such as (Ga,Mn)As are particularly favorable materials in this research area for their rich phenomenology of magnetoresistive characteristics and the potential to combine and integrate spintronics with conventional semiconductor microelectronics [1, 2]. Only a few works have so far reported electrical gating, via charge depletion, of magnetic properties of (III,Mn)V ferromagnetic semiconductor field-effect transistors (FETs). Curie temperature and coercive field variations have been demonstrated by applying tens of volts on a top-gate FET with an oxide dielectric separating a metal gate from an (In,Mn)As or (Ga,Mn)As channel [3]–[6]. The difficulty to achieve efficient depletion in the highly doped ferromagnetic semiconductor films has motivated research in several alternative routes to the field-control of magnetism in (Ga,Mn)As, including the electro-mechanical gating by piezo-stressors [7]–[9] or fabrication of small island Coulomb blockade transistors with magnetization-dependent single-electron charging energy [10]. In this paper, we introduce an all-semiconductor, epitaxial p–n junction FET [11] allowing for a large depletion of (Ga,Mn)As thin films at a few volts. We demonstrate various gatable magnetic characteristics ranging from the anisotropic magnetoresistance (AMR) and the Curie temperature to coercivity and magnetization switchings induced by short electrical pulses.

2. Device structure and simulations

The schematic cross-section of the III–V heterostructure used in our study is shown in figure 1(a). It is a semiconductor p–n junction FET specially designed to accommodate ferromagnetism in the p-type region and its efficient depletion by low voltages. From the top, the structure comprises a 5 nm thick approximately 2.5% Mn-doped GaAs capped by 2 nm of undoped GaAs to prevent oxidation of the underlying transition metal-doped semiconductor film. These two top layers were grown by low-temperature molecular-beam epitaxy (MBE) to avoid Mn precipitation. The 2.5% doping was chosen to pass the insulator-to-metal transition threshold which for the moderately deep Mn_{Ga} acceptor is between 1 and 2% and to achieve a robust ferromagnetic state with Curie temperature $T_c \approx 30$ K, while still minimizing the number of unintentional interstitial-Mn impurities [1, 2, 12]. (The interstitial Mn is highly mobile at the growth temperature and its diffusion into the p–n junction would result in detrimental leakage

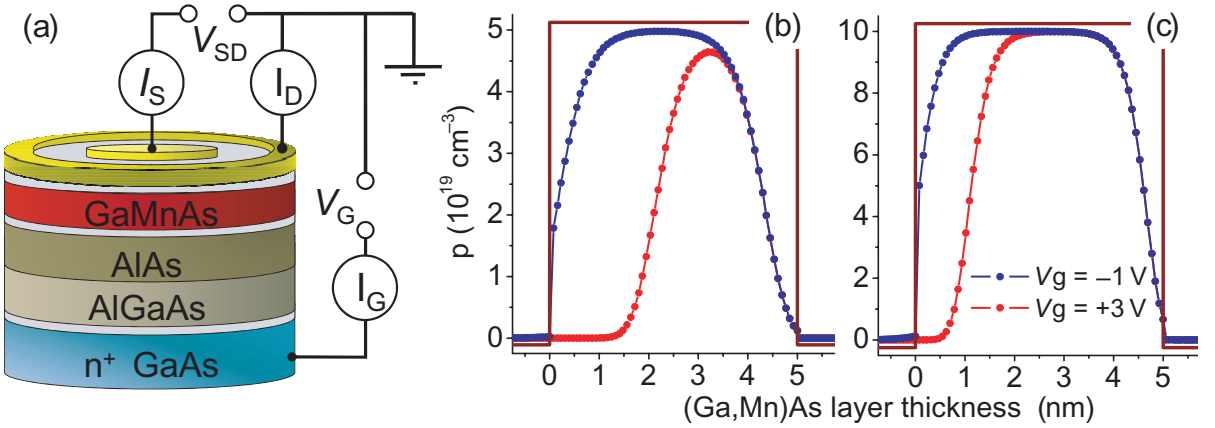

Figure 1. (a) Schematic of the ferromagnetic p–n junction FET structure and the Corbino disk geometry of the source and drain contacts. (b) and (c) Numerical simulations of the hole density profile at −1 V (accumulation) and +3 V (depletion), considering a 2×10^{19} cm^{-3} electron doping in the n-GaAs and 5×10^{19} and 10^{20} cm^{-3} hole doping in the p-(Ga,Mn)As.

currents.) The Curie temperature measured by SQUID in an unpatterned piece of the wafer is comparable to maximum T_c's achieved at the same Mn-doping in thicker films, indicating a very good quality of our ultra-thin ferromagnetic semiconductor epilayer.

The n-type gate electrode is formed by a highly Si-doped (2×10^{19} cm^{-3}) GaAs grown by high-temperature MBE. The large electron doping is required in order to achieve appreciable and voltage-dependent depletion of the ferromagnetic p-region with hole doping $\sim 10^{20}$ cm^{-3}. The built-in electrostatic barrier due to the depletion effect at the p–n junction is further supported by inserting a 10 nm $Al_{0.3}Ga_{0.7}As$ spacer layer with a large conduction band off-set to the neighbouring n-GaAs and a 10 nm AlAs spacer with a large valence band off-set to the neighbouring p-(Ga,Mn)As.

Self-consistent numerical simulations, shown in figure 1(b), confirm that sizable depletions are achievable by gating our heterostructure with less than 4 V. The calculations also illustrate that total hole depletion/accumulation in the (Ga,Mn)As contains both the change in the average 3D hole density in the epilayer and the change in the effective thickness of the conductive ferromagnetic semiconductor film. The Drude channel conductance is linearly proportional to both of these components and is therefore expected to be linearly proportional to the total depletion/accumulation. Measurements discussed below were done at voltages between −1 V (forward bias) and +3 V (reverse bias) for which the leakage currents between the n-GaAs gate and p-(Ga,Mn)As channel were more than two orders of magnitude smaller than the channel currents. The (Ga,Mn)As channel was lithographically patterned in a low-resistance Corbino disk geometry with the inner contact diameter of 500 μm and the outer diameter of 600 μm.

3. Voltage control of Curie temperature and magnetoresistance

In figure 2(a), we plot the measured channel resistances versus gate voltage at temperature 4–40 K. At 40 K, we observe an increase of the channel resistance at positive voltages by approximately 25%. It is consistent with the depletion of the (Ga,Mn)As channel as predicted by

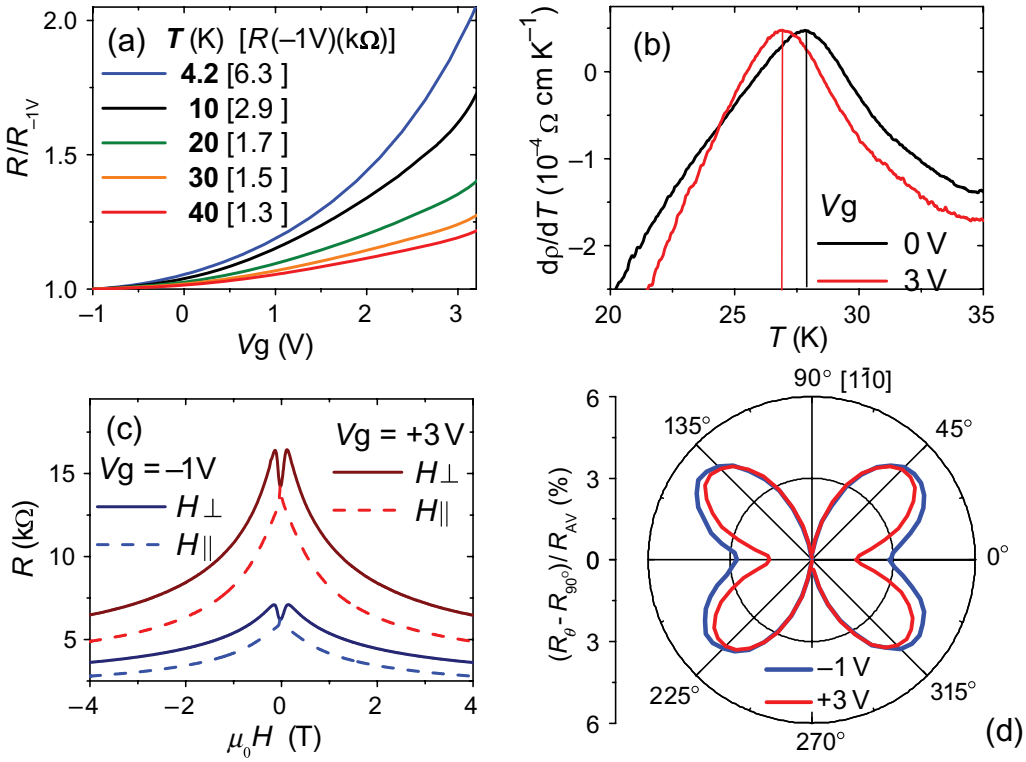

Figure 2. (a) Gate voltage dependence of the p-(Ga,Mn)As channel resistance at temperatures 4–40 K. (b) Temperature derivative of the measured channel resistivity at 0 and +3 V. The maximum corresponds to T_c. (c) In-plane ($H_\parallel$) and perpendicular-to-plane ($H_\perp$) magnetic field-sweep measurements of the channel resistance at −1 and +3 V. The difference between the $H_\parallel$ and $H_\perp$ sweeps above the reorientation field of ≈150 mT corresponds to the out-of-plane AMR. (d) In-plane AMR measured at saturation (4 T) in a rotating in-plane field at −1 and +3 V. R_{AV} is the average channel resistance measured across the entire angular range for the respective gate voltages.

the simulations in figure 1(b). At low temperatures, the gating effect is strongly enhanced; at 4 K the increase of R between −1 and +3 V is by more than 100%. We attribute this enhancement to the vicinity of the metal–insulator transition in our ultra-thin (Ga,Mn)As epilayer.

In figure 2(b), we show the voltage dependence of the Curie temperature in the ferromagnetic p–n junction. Our measurement technique is distinct from previous studies, which relied on approximate extrapolation schemes based on Arrot plot measurements at finite magnetic fields [3, 5, 13]. Recent observation and interpretation by the authors [14] of the peak in the zero-field temperature derivative of the resistance at the Curie point in good-quality (Ga,Mn)As materials has provided the tool for direct transport measurements of T_c in microdevices without relying on any extrapolation schemes. In figure 2(b), we plot differentiated resistivity curves obtained in our device at 0 and +3 V. The data show a clear shift of the Curie temperature, i.e. the magnetization can be turned on and off in parallel with accumulating and depleting holes in the ferromagnetic semiconductor channel by biasing the p–n junctions with a few volts.

Curie temperature variations provide the key physical demonstration of the low-voltage control of magnetization. Nevertheless, for most spintronic functionalities it is not required to destroy the ordered state of spins but only to change their collective orientation. We therefore focus on effects related to reorientations of the unit vector of the macroscopic moment. To avoid thermal fluctuations of the magnetization, all measurements are done far from the Curie point at 4 K.

In figure 2(c), we show magnetoresistance traces recorded during in-plane and perpendicular-to-plane sweeps of an external magnetic field, at gate voltages of −1 and +3 V. Apart from the negative isotropic magnetoresistance (IMR), the data indicate a remarkably large AMR effect which at saturation reaches ∼30%. (Note that AMR sensors fabricated in transition metal ferromagnets with AMR ratios of a few per cent [15] marked the dawn of spintronics in the early 1990s.) The resistance is larger for the perpendicular-to-plane magnetization orientation and the size of the effect is enhanced by depletion. The electrical response of our system to magnetization rotations is both large and tuneable by low gate voltages.

The magnetoresistance traces in figure 2(c) indicate that the film has a magnetic anisotropy favoring in-plane magnetization, which is overcome by an external field of approximately 150 mT. At weaker magnetic fields, magnetization switching effects are confined to the plane of the ferromagnetic film. The qualitative nature of the in-plane magnetic anisotropy landscape, which determines the switching processes, can be scanned in our Corbino microdevice by recording the AMR at a rotating in-plane saturation field. Unlike in the out-of-plane rotation AMR, contributions depending on the relative angle between the in-plane magnetization and current average out over the radial current lines. The in-plane AMR then depends purely on the angle between magnetization and crystallographic axes [16]. It reflects therefore the same underlying symmetry breaking crystal fields as the magnetic anisotropy. The measurements, shown in figure 2(d), unveil a cubic anisotropy along the [110]/[1$\bar{1}$0] crystal axes and an additional uniaxial term breaking the symmetry between the [110] and [1$\bar{1}$0] directions. Although the specific responses to these symmetries can be very different for the AMR and for the magnetic anisotropy, the presence of the cubic and uniaxial AMR terms and their sensitivity to the gate voltage observed in figure 2(d) suggest that the in-plane magnetization orientation itself can be switched at weak magnetic fields by the low-voltage charge accumulation or depletion.

4. Persistent magnetization switching with short voltage pulses

A variable width of hysteretic magnetization loops measured at different constant gate voltages, shown in figure 3(a), is the prerequisite for observing electrically assisted magnetization switchings. Note that electrical measurements of magnetization reorientations utilized in figures 3 and 4 are facilitated in our system by the IMR which responds to abrupt changes of the total magnetic induction upon a 180° reversal, and by a combined effect of the IMR and of the AMR for intermediate switchings by less than 180°. The amplitude of the AMR and the IMR contributions is similar in our experiments. The switchings by short low-voltage pulses are demonstrated in figure 3(b) and analyzed in detail in figure 4. The experiments were performed at constant field-sweep rate of 0.1 mT s^{-1} starting from negative saturation field of 1 T. The gate voltage was set to a base value of −1 V and then after each measurement step spanning 1 s we applied a 10 ms voltage pulse of a fixed magnitude and then returned to the base voltage.

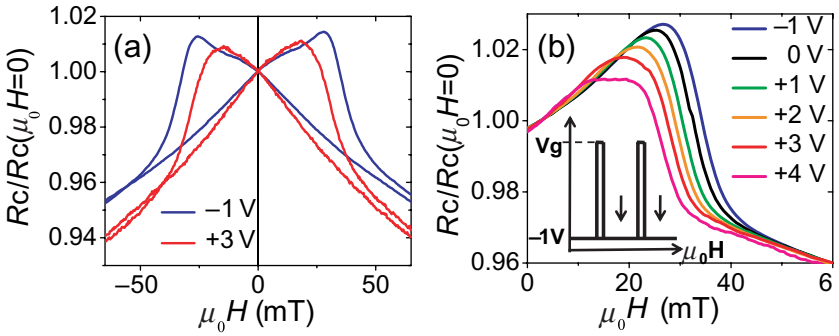

Figure 3. (a) Hysteretic field-sweep measurements at field angle $\theta = 90^\circ$ for constant gate voltages of -1 and +3 V. (b) Up-sweeps of the $\theta = 90^\circ$ in-plane field at constant -1 V gate voltage, and for measurements with the gate voltage set to a base value of -1 V and with short additional voltage pulses corresponding to a total peak voltage of 0, +1, +2, +3 and +4 V, respectively.

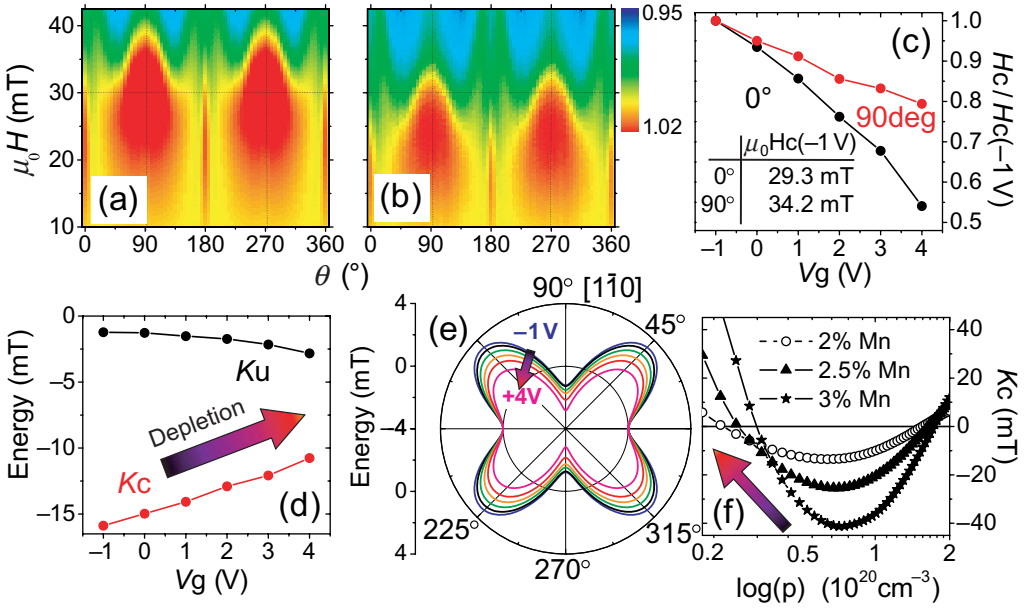

Figure 4. (a) and (b) Color maps of channel resistance as a function of the in-plane field angle and magnitude (normalized to $H = 0$ resistance) for -1 V constant voltage and +3 V peak voltage measurements, respectively. (c) Switching fields at field angles $\theta = 0^\circ$ has a stronger suppression than at 90° as a function of the gate voltage. (d) Uniaxial and cubic anisotropy constants and (e) corresponding anisotropy energy profiles derived from the measured $\theta = 0^\circ$ and 90° switching fields. (f) Microscopic calculations of the cubic anisotropy constant. Arrows in (d) and (f) highlight the common trend with depletion.

The technique allows us to demonstrate magnetic response to short electric pulses and the persistence of induced reorientations of the magnetization vector. It also removes potentially obscuring variations among the resistance traces in regions away from magnetization switchings, which are caused by different slopes of the negative IMR at different gate voltages.

In figure 3(b), we compare measurement with no pulses (constant −1 V gate voltage) and data acquired at 0 to +4 V peak voltages. The field was swept along the $[1\bar{1}0]$ crystal direction ($\theta = 90^\circ$, where θ is the in-plane field angle measured from the [110] direction). As argued in detail in figure 4 and confirmed by SQUID magnetization measurements on an unpatterned part of the wafer, the $[1\bar{1}0]$ direction is the main magnetic easy axis. The negative IMR then allows us to observe the drop in R corresponding to a 180° reversal from an antiparallel to a parallel configuration of field and magnetization and a corresponding increase of the magnetic induction. As the applied peak voltage increases, the magnetization reversals consistently shift to lower magnetic fields and the magnetization remains switched when the peak voltage pulse is turned off.

5. Theoretical discussion

To discuss the detailed phenomenology of these persistent low-voltage-induced magnetization switchings, we present in figures 4(a) and (b) field-sweep measurements at fixed field angles spanning the whole interval in 5° steps. In panels (a) and (b), we show color maps of the resistance as a function of the field magnitude and angle for −1 V constant voltage and for the +3 V peak-voltage measurements, respectively. The main effect observed in these plots is the overall suppression of the magnitude of the switching fields by depletion. Additionally, the relative suppression is stronger at $\theta = 0^\circ$ than at 90°, as highlighted in figure 4(c). This indicates that both the magnitude and ratio between the uniaxial and cubic anisotropy fields are modified by the gate voltage. To quantify the depletion-induced modification of the magnetic anisotropy, we extracted the anisotropy constants from fitting the measured $\theta = 0^\circ$ and 90° switching fields to a single domain anisotropy energy model, $E(\theta, \phi) = K_u \sin^2\phi - K_c \sin^2 2\phi/4 - MH \cos(\theta - \phi)$, where H and M are the magnitudes of the external field and magnetization, respectively, and ϕ is the magnetization angle. This simple model gives the lower bound for the anisotropy constants. The uniaxial constant K_u is relatively weak compared with the cubic constant K_c, as shown in figure 4(d). They both have a negative sign corresponding to the magnetic easy directions along the $[1\bar{1}0]$ and [110] axes and the most easy direction along the $[1\bar{1}0]$. As shown also from figure 4(d), the dominant effect of depletion is in reducing the magnitude of K_c. Figure 4(e) shows how the corresponding anisotropy energy profiles at $H = 0$ evolve with depletion.

We now discuss the key experimental observations by employing the $\mathbf{k}\cdot\mathbf{p}$ semiconductor theory approach combined with the mean-field kinetic-exchange model of hole-mediated ferromagnetism in (Ga,Mn)As [1, 2]. Calculations for 2.5% local moment doping and hole density $p \sim 1 \times 10^{20}\,\mathrm{cm}^{-3}$, for which the simulations in figure 1(b) predict hole depletions consistent with the measured variations of the channel resistance at temperatures near T_c, yield $T_c \sim 20\,\mathrm{K}$ and $\mathrm{d}T_c/\mathrm{d}p \approx 1 \times 10^{-19}\,\mathrm{K\,cm}^3$. Both the absolute value of the Curie temperature and the few Kelvin suppression of T_c at a ∼20% hole depletion predicted by the theory are consistent with our p–n junction simulations and the measured gate-dependent T_c values.

The semiconductor theory modelling, which includes strong spin–orbit coupling effects in the host semiconductor valence band, also captures the sensitivity of magnetocrystalline anisotropies in (Ga,Mn)As to hole density variations. The cubic anisotropy is included by accounting in the $\mathbf{k}\cdot\mathbf{p}$ model for the zincblende crystal structure of GaAs. The additional weak uniaxial anisotropy is often present in (Ga,Mn)As epilayers but its microscopic origin is not known and we will therefore focus only on the stronger cubic anisotropy term. As

shown in figure 4(f), the microscopically calculated K_c constant changes sign at hole density of approximately 1.5×10^{20} cm^{-3}. Below this density it favors the [110]/[1$\bar{1}$0] magnetization directions, consistent with the experimental data. The typical magnitudes of K_c of ∼10 mT are also consistent with experiment and considering the large gate action seen at low temperatures we can also associate, semiquantitatively, the decreasing magnitude of the experimental K_c at depletion with the behavior of the theoretical K_c at low hole densities.

To conclude, we have reported low-voltage control of magnetic properties of a p–n junction FET via depletion effect in the ferromagnetic semiconductor channel. We have shown variable T_c and AMR, and demonstrated magnetization switchings induced by short electric field pulses of a few volts. Our concept of the spintronic transistor is distinct from previously demonstrated high-voltage metal-oxide–semiconductor ferromagnetic FETs [3, 5, 13] or electro-mechanically gated ferromagnets by piezo-stressors [7]–[9], [17]–[20]. It is realized in an all-semiconductor epitaxial structure and offers a principally much faster operation. In basic physics research, we expect broad utility of our results in studies of carrier-mediated ferromagnetism and in interdisciplinary fields combining ferromagnetism and spin–orbit coupling effects with localization and quantum-coherent transport phenomena [21] controlled by carrier depletion.

Acknowledgments

We acknowledge helpful discussions with R P Campion, M Cukr, B L Gallagher, M Maryško, J Sinova and J Zemek, and from EU Grant IST-015728, FP7 Project 214499 NAMASTE, from Czech Republic Grants FON/06/E001, FON/06/E002, AV0Z1010052, KAN400100652 and LC510, and from US Grant SWAN-NRI.

Note added in proof. Our work was completed [22] prior to the publication of the related and independent work on electrostatically controlled magnetic anisotropy in a thin (Ga,Mn)As layer, reported in [6].

References

[1] Matsukura F, Ohno H and Dietl T 2002 Ferromagnetic semiconductors ed K H J Buschow *Handbook of Magnetic Materials* vol 14 p 1 (Amsterdam: Elsevier)

[2] Jungwirth T, Sinova J, Mašek J, Kučera J and MacDonald A H 2006 Theory of ferromagnetic (III,Mn)V semiconductors *Rev. Mod. Phys.* **78** 809

[3] Ohno H, Chiba D, Matsukura F, Omiya T, Abe E, Dietl T, Ohno Y and Ohtani K 2000 Electric-field control of ferromagnetism *Nature* **408** 944

[4] Chiba D, Yamanouchi M, Matsukura F and Ohno H 2003 Electrical manipulation of magnetization reversal in a ferromagnetic semiconductor *Science* **301** 943

[5] Chiba D, Matsukura F and Ohno H 2006 Electric-field control of ferromagnetism in (Ga,Mn)As *Appl. Phys. Lett.* **89** 162505

[6] Chiba D, Sawicki M, Nishitani Y, Nakatani Y, Matsukura F and Ohno H 2008 Magnetization vector manipulation by electric fields *Nature* **455** 515

[7] Rushforth A W *et al* 2008 Voltage control of magnetocrystalline anisotropy in ferromagnetic-semiconductor/piezoelectric hybrid structures *Phys. Rev.* B **78** 085314

[8] Overby M, Chernyshov A, Rokhinson L P, Liu X and Furdyna J K 2008 GaMnAs-based hybrid multiferroic memory device *Appl. Phys. Lett.* **92** 192501

[9] Goennenwein S T B, Althammer M, Bihler C, Brandlmaier A, Geprägs S, Opel M, Schoch W, Limmer W, Gross R and Brandt M S 2008 Piezo-voltage control of magnetization orientation in a ferromagnetic semiconductor *Phys. Status Solidi* **2** 96

[10] Wunderlich J *et al* 2006 Coulomb blockade anisotropic magnetoresistance effect in a (Ga,Mn)As single-electron transistor *Phys. Rev. Lett.* **97** 077201

[11] Boukari H, Kossacki P, Bertolini M, Ferrand D, Cibert J, Tatarenko S, Wasiela A, Gaj J A and Dietl T 2002 Light and electric field control of ferromagnetism in magnetic quantum structures *Phys. Rev. Lett.* **88** 207204

[12] Jungwirth T *et al* 2007 Character of states near the Fermi level in (Ga,Mn)As: impurity to valence band crossover *Phys. Rev.* B **76** 125206

[13] Stolichnov I, Riester S W E, Trodahl H J, Setter N, Rushforth A W, Edmonds K W, Campion R P, Foxon C T, Gallagher B L and Jungwirth T 2008 Nonvolatile ferroelectric control of ferromagnetism in (Ga,Mn)As *Nat. Mater.* **7** 464

[14] Novák V *et al* 2008 Curie point singularity in the temperature derivative of resistivity in (Ga,Mn)As *Phys. Rev. Lett.* **101** 077201

[15] McGuire T and Potter R 1975 Anisotropic magnetoresistance in ferromagnetic 3d alloys *IEEE Trans. Magn.* **11** 1018

[16] Rushforth A W *et al* 2007 Anisotropic magnetoresistance components in (Ga,Mn)As *Phys. Rev. Lett.* **99** 147207

[17] Kim S-K, Lee J-W, Shin S-C, Song H W, Lee C H and No K 2003 Voltage control of a magnetization easy axis in piezoelectric/ferromagnetic hybrid films *J. Magn. Magn. Mater.* **267** 127

[18] Lee J-W, Shin S-C and Kim S-K 2003 Spin engineering of CoPd alloy films via the inverse piezoelectric effect *Appl. Phys. Lett.* **82** 2458

[19] Botters B, Giesen F, Podbielski J, Bach P, Schmidt G, Molenkamp L W and Grundler D 2006 Stress dependence of ferromagnetic resonance and magnetic anisotropy in a thin NiMnSb film on InP(001) *Appl. Phys. Lett.* **89** 242505

[20] Boukari H, Cavaco C, Eyckmans W, Lagae L and Borghs G 2007 Voltage assisted magnetic switching in $Co_{50}Fe_{50}$ interdigitated electrodes on piezoelectric substrates *J. Appl. Phys.* **101** 054903

[21] Neumaier D, Wagner K, Geissler S, Wurstbauer U, Sadowski J, Wegscheider W and Weiss D 2007 Weak localization in ferromagnetic (Ga,Mn)As nanostructures *Phys. Rev. Lett.* **99** 116803

[22] Owen M H S *et al* 2008 Low voltage control of ferromagnetism in a semiconductor p–n junction arXiv:0807.0906 [cond-mat]